Identification of Railway Bridges Using Traffic-Induced Vibrations

E. UZGIDER, A. K. ŞANLI, F. PIROĞLU, AND B.Ö. ÇAĞLAYAN

A program of full-scale bridge tests was undertaken as a principal part of the research project entitled Rehabilitation of Old Railway Bridges and primarily considered railway bridges located on the Turkish Railway Network. This program was financially supported by the North Atlantic Treaty Organization Science for Stability Program. Bridges were tested during the summers of 1991, 1992, 1993, and 1994. The test program followed a standard pattern for each bridge. An efficient damage detection procedure developed in the course of TU-BRIDGE research studies with application to the Çerkezköy Railway Bridge is described.

A research project entitled Rehabilitation of Old Railway Bridges and started on February 1990, was financially sponsored by the North Atlantic Treaty Organization (NATO) Science for Stability Program with the code name TU-850-BRIDGES. The main objective of this research program was to evaluate current structural conditions and reliability of these bridges, which are the most important part of the Turkish railway system. Repairing and strengthening procedures will be developed as needed.

In the framework of the TU-BRIDGES Project a rational procedure has been developed to detect any existing damage and deterioration globally on old railway bridges using collected acceleration data during their dynamic field test. Because labor needed to install acceleration transducers is considerably easier than that needed to install strain transducers, in less than one day the needed data can be collected, avoiding the costly rail traffic shutdowns. Thus, the procedure could be a tool for enhancing bridge inspection and identifying globally existing damages with their location. If global damage is detected for any bridge region, then the process must be completed by strain measurements focused on that region to achieve an element-level damage detection.

To avoid the rail traffic shutdowns of forced vibration test techniques, an ambient vibration technique in which a bridge structure is excited by the current rail traffic is used. The added mass effect of the bridge traffic is avoided by considering the acceleration data recorded after the train has left the bridge. Several previous studies (*1–5*) showed that current traffic is considered as an excitation mechanism.

Not all degrees of freedom can be measured during a test because an unreasonable amount of transducers are needed and, thus, not all modes are observed in the response records. On the other hand, adequate control of excitation, which is only the case for forced vibration tests under laboratory conditions, is essential for precise mode shape measurements, but it is not the case for the traffic-induced vibration tests performed on the real bridge structures. Thus, instead of considering element-level identification, stiffness parameters representing the stiffness changes in the selected structural segments containing some amount of structural members, can be defined more reliably, depending on the identified modal parameters.

The proposed method has been successfully employed for the data recorded from the 11 railway bridges tested within the framework of the TU-BRIDGES Project. The total process that is offered to follow to achieve element-level damage detection is described in Figure 1.

Department of Civil Engineering, Istanbul Technical University, 80626 Maslak, Istanbul, Turkey.

GLOBAL DAMAGE DETECTION METHOD

The proposed method consists of two main consecutive phases: (a) modal identification and (b) segmentary stiffness identification.

Modal Identification

After preprocessing the recorded acceleration data to eliminate possible noise contamination and removing existing trends and outliers as given in detail elsewhere (*6,7*), using the well-known spectral analysis method similar to that used by Felber (*5*), modal parameters are defined on the basis of the acceleration data recorded after the train has left the bridge.

Segmentary Stiffness Identification

Distress in civil engineering structures often may have a significant effect on stiffness, but not on mass. In steel structures, fatigue cracks reduce stiffness without loss of mass, and even a corrosion loss will affect stiffness to a much greater extent than it will affect mass. Thus, it is safely assumed that because of these structural damages, mass values are not changed. Then, stiffness identification can be used as an efficient tool to detect the structural changes with respect to the computer model. A dominant part of these changes may be assumed to be caused by the existing damages in the structure, if an accurate computer modeling technique has been employed during the identification process. On the other hand, a considerable simplification is possible in stiffness identification when the function of a member in a structure relies primarily on one stiffness. For example, floor beams in the bridge provide primarily flexural stiffness, whereas truss members provide primarily axial stiffness. In such cases, damage in a member will influence modal parameters through the primary stiffness only, and the change in a member stiffness may be represented by the change in its elasticity modulus. However, stiffness changes are not sensitive enough to small structural damages such as those caused by fatigue cracks or corrosion loss existing on a bridge member.

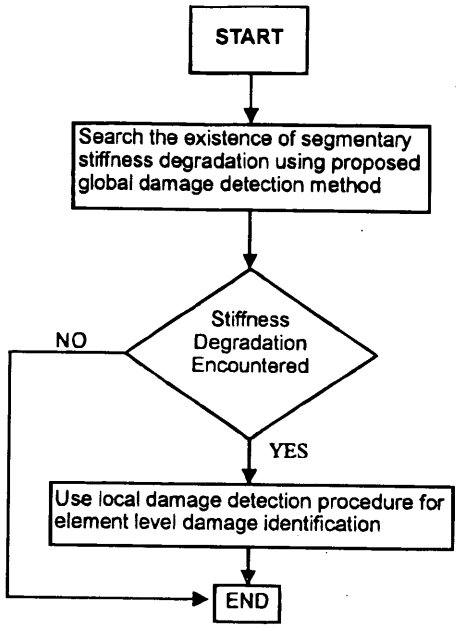

FIGURE 1 Element-level identification procedure.

Thus, instead of considering bridge members one by one, upper and lower lateral bracing system, two plane trusses, and vertical and longitudinal support springs of the bridge were divided into a set of segments in this identification process. The segmentation pattern employed in this study is shown in Figure 2. Then, the modulus of elasticity of each characteristic region is considered as the segmentary stiffness parameters to be identified. Then, a negative percent change of identified elasticity modulus of any segment with respect to the original value will be interpreted as the signature of the total stiffness degradation or damage occurring in the members covered by this segment. On the other hand, positive percent changes are considered as the result of the other sources of stiffness that cannot be incorporated into the computer model.

To estimate the segmentary stiffness parameters the weighted squares of the difference between the experimentally identified and computed modal parameters, subject to limits on the extreme values of the segmentary stiffness parameters will be minimized. The following is the associated constrained nonlinear optimization problem for the proposed least-squares estimator:

$$\underset{\boldsymbol{E}}{\text{minimize}}\ J(\boldsymbol{E}) = \sum_{i=1}^{n} gi\,[MMP_i - CMP_i(\boldsymbol{E})]^2 \tag{1}$$

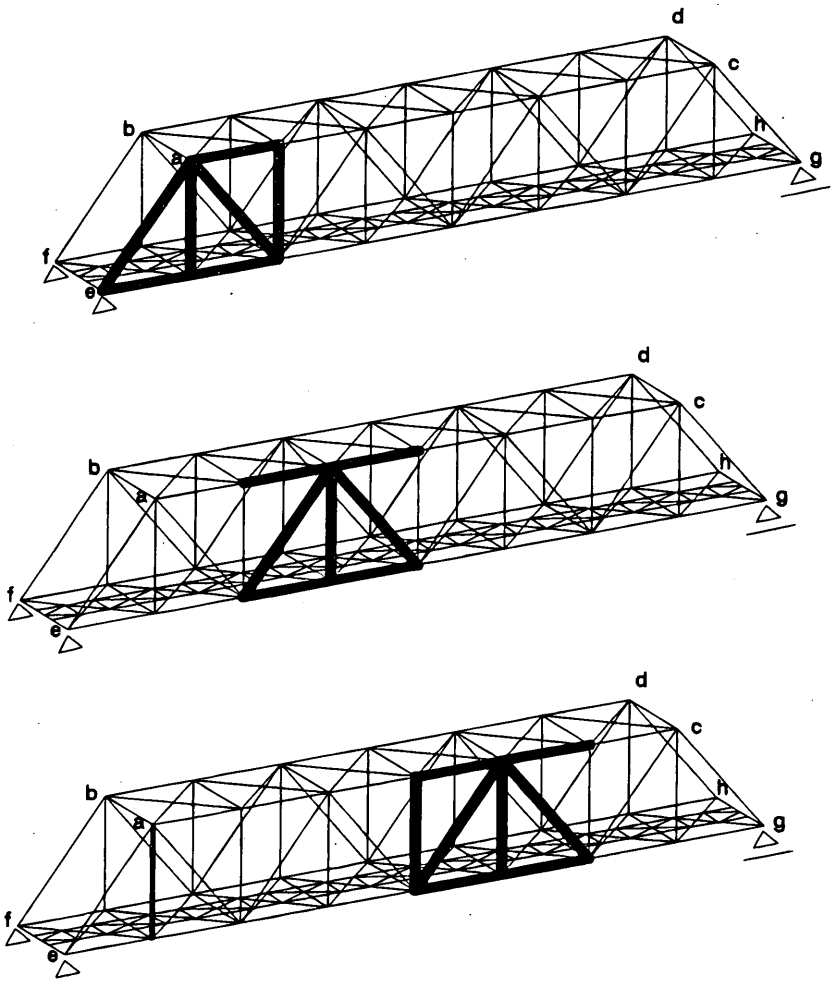

FIGURE 2 Structural segmentation.

subject to $\boldsymbol{E}^l \leq \boldsymbol{E} \leq \boldsymbol{E}^u$ where $\boldsymbol{E}$ is the segmentary stiffness parameter vector,

$$\boldsymbol{E} = \{E_1, E_2, \ldots, E_m\}^T \quad (1a)$$

MMP_i is the experimentally identified or measured modal parameters and n is the number of experimentally identified or measured modes. The vectors $\boldsymbol{E}^l$ and $\boldsymbol{E}^u$ are the lower and upper limit vectors, respectively, for the unknown segmentary stiffness parameters, and the inequalities are enforced component by component. These limits are available to enforce known characteristics of the stiffness parameters. For example, one might know in advance that a negative value in the modulus of elasticity is impossible on physical grounds, and the stiffness parameters are limited from above. These limits define the feasible region and are important because they eliminate the possibility of converging to physically unreasonable solutions. For this problem, the upper limit might be set as some multiple of nominal design values or expected parameter values to control the algorithm.

The weight g_i reflects the relative confidence in the test data. In this study, cross-correlation coefficients calculated between the data collected from the different measuring points of the bridges are employed as the weight. CMP_i $(\boldsymbol{E})$ stands for a set of scalar cubic functions simulating the variation of modal parameters with respect to the segmentary stiffness parameters. These scalar functions can be obtained in a way similar to that employed by Douglas and Reid (*8*).

A three dimensional finite element computer model covering all the geometric irregularities and stiffness changes existing on the considered bridge structure is employed for the free vibration analyses, in which consistent mass is employed for the bridge members. Point mass approximation is used for the mass contribution from nonstructural components such as sleepers, rails, or walkways, and so forth. Four vertical and two horizontal spring elements are also used to simulate the effective vertical stiffness of the combined bearing and abutment structure and the longitudinal restraints at the sliding bearings.

The following is a simple representation of the modal parameters as the cubic functions of the segmentary stiffness parameters used in this study:

$$CMP_i = A_i + \sum_{j=1}^{m} [B_{ij} \cdot E_j + C_{ij} \cdot E_j^2 + D_{ij} \cdot E_j^3] \qquad i = 1, \ldots, n \quad (2)$$

where

n and m = total number of parameters and total number of structural segments to be considered, respectively,
E_j = the jth segmentary stiffness parameter, and
A, B, C, and D = unknown constants to be determined.

Thus, to determine these constants, three different-level perturbations are given to the segmentary stiffness parameters in addition to their initial values:

$$E_{oj} = E \quad (2a)$$

$$E_{kj} = E + (\delta E)_k \qquad j = 1, \ldots, m \qquad k = 1, \ldots, 3 \quad (2b)$$

Then, by employing the aforementioned sophisticated computer model of the considered bridge, a set of free vibration analyses is performed for the initial segmentary stiffness values (Equation 2*a*) and for the three levels of segmentary stiffness perturbations given in Equation 2*b* considered sequentially for each segment. In this way, totally $\{n \times (m + 1)\}$ modal parameters are produced. To determine unknown constants of Equation 2, by employing these modal parameters the following equations can be written:

$$CMP_i^{(0)} = A_i + \sum_{j=1}^{m} [B_{ij} \cdot E_{oj} + C_{ij} \cdot E_{oj}^2 + D_{ij} \cdot E_{oj}^3] \quad (3)$$

$$CMP_{i,1}^{(k)} = A_i + B_{i1} \cdot E_{k1} + C_{i1} \cdot E_{k1}^2 + D_{i1} \cdot E_{k1}^3 + \sum_{j=2}^{m} [B_{ij} \cdot E_{oj} + C_{ij} \cdot E_{oj}^2 + D_{ij} \cdot E_{oj}^3] \quad (3a)$$

$$\vdots$$

$$CMP_{i,m}^{(k)} = A_i + \sum_{j=1}^{m-1} [B_{ij} \cdot E_{oj} + C_{ij} \cdot E_{oj}^2 + D_{ij} \cdot E_{oj}^3] + B_{im} \cdot E_{km} + C_{im} \cdot E_{km}^2 + D_{im} \cdot E_{km}^3 \qquad i = 1, \ldots, n \qquad k = 1,2,3 \quad (3b)$$

where $CMP_i^{(0)}$ is the ith modal parameter obtained by free vibration analysis for the initial segmentary stiffness values and $CMP_{i,m}^{(k)}$ is the ith modal parameter obtained by the same analysis for kth-level perturbed segmentary stiffness values of bridge segment m only. In this way, $\{n \times m \times (k = 3) + n\}$ linear equations can be produced for the same amount of unknowns. After having defined unknown coefficients of the cubic functions given in Equation 2, the constrained nonlinear optimization problem defined in Equation 1 can be solved to obtain unknown segmentary stiffness parameter values using any of a number of available optimization methods. In this study a sequential quadratic programming (SQP) method is used. An overview of SQP has been given by Fletcher (*9*), Gill et al. (*10*), and Hock and Schittowski (*11*).

As was previously discussed (*12*), nonlinear optimization algorithms usually give results that are strongly affected by the topography of the scalar error function J given in Equation 1. If this function has more than one local minimum, then the initial estimate made at the start for segmentary stiffness parameters controls the convergence of the algorithm to one of these local minima. In this study, to prevent the convergence of the algorithm to the local minima other than the true one, the bounding constraints are imposed on the segmentary stiffness parameters as explained earlier (Equation 1). On the other hand, a different rate of sensitivity of the modal parameters to the segmentary stiffness parameters makes the basin of attraction around the true local minimum a narrow valley with steep slopes for some of the segmentary stiffness parameters and shallow slopes for the rest. Consequently, the algorithm will not be able to easily reach the bottom of this valley or the local minimum. To cure the numerical difficulties caused by this problem, all the segmentary stiffness parameters were scaled depending on the rate of sensitivity of the modal parameters to them. Obviously, this transforms the shallow slopes that are associated with some of the segmentary stiffness parameters to steep enough slopes to eliminate the numerical problem. To perform such a scaling, the following coordinate transformation is used in this study:

$$\theta_j \cdot E_j = \overline{E}_j \quad (4)$$

in which θ_j is RMS of the jth column of the following sensitivity matrix:

$$S = \begin{bmatrix} \theta_{11}^{(k1)} & \theta_{12}^{(k1)} & \dots & \theta_{1m}^{(k1)} \\ \theta_{21}^{(k2)} & \theta_{22}^{(k2)} & \dots & \theta_{2m}^{(k2)} \\ \cdot & \cdot & \dots & \cdot \\ \cdot & \cdot & \dots & \cdot \\ \cdot & \cdot & \dots & \cdot \\ \theta_{n1}^{(kn)} & \theta_{n2}^{(kn)} & \dots & \theta_{nm}^{(kn)} \end{bmatrix} \begin{matrix} \downarrow \\ i = 1, \dots, n \end{matrix} \qquad (4a)$$

$$j = 1, \dots, m \rightarrow$$

$$\theta_j = \left(\frac{1}{n} \times \sum_{i=1}^{n} \theta_{ij}^{(ki)^2} \right)^{\frac{1}{2}} \qquad (4b)$$

Where

n and m = total number of modal parameters considered and total number of structural segments, respectively;

ki = segment number whose stiffness changes most affect the ith modal parameter's value; and

$\theta_{ij}^{(ki)}$ = dimensionless constant that can be expressed, depending on Equation 2, as follows:

$$\theta_{ij}^{(ki)} = \frac{\left(\frac{\partial CMP_i}{\partial E_j} \right)}{\left(\frac{\partial CMP_i}{\partial E_{ki}} \right)} \qquad (4c)$$

where $0 < \theta_{ij}^{(ki)} \leq 1$, $i = 1, \dots, n$; and $j = 1, \dots, ki, \dots, m$.

Experimental Verification of Method

To check the validity and efficiency of the proposed method, laboratory tests were performed for the simply supported steel beam model, part of which was braced by a steel plate in Segment 2. In the laboratory test, the test data acquisition system is Keithley 500 with 16 A/D channels, having a total sampling rate of 50,000 sps and coupled to a Toshiba T3200 laptop computer having a 16-MHz 80386 processor, 9 MByte RAM, and 40-MByte hard disk capacities. Accelerations were recorded at seven equally spaced locations on the beam by single-axial accelerometers made by Terra Technology Corporation. The beam model was excited by a pull-down and quick-release procedure. A schematic of the equipment setup is shown in Figure 3. After the collected acceleration data were preprocessed, the first flexural mode parameters were identified, (Table 1), along with the others computed using COSMOS/M Finite Element Software (*13*) by employing the computer model of the tested beam described in Figure 4.

The flexural stiffness change in Segment 2 can be reflected in the modulus of elasticity as follows:

$$E_2 = (I_2/I_1) * E$$

where $I_2 = 14.31$ cm^4 and $I_1 = 8.63$ cm^4 are the moments of inertia of the braced and regular cross sections, respectively. Thus,

$$E_2 = 1.6582\, E = 34\,820 \text{ kN/cm}^2$$
$$E_1 = E_3 = E_4 = E_5 = 21\,000 \text{ kN/cm}^2$$

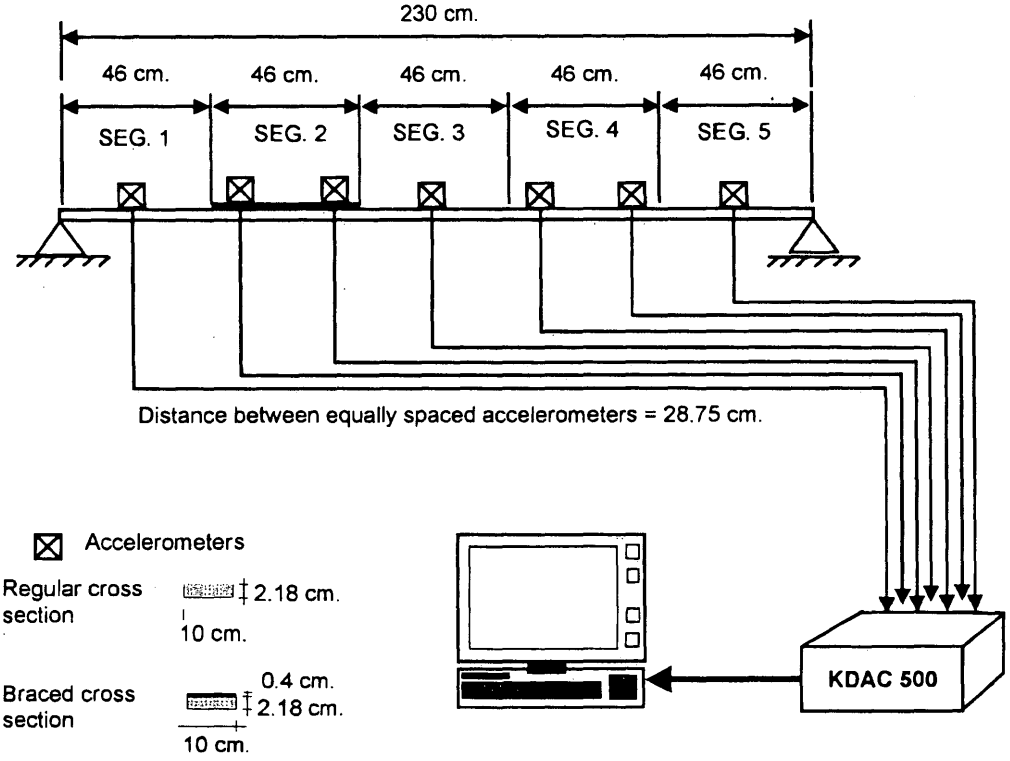

FIGURE 3 Laboratory test setup.

TABLE 1 First Flexural Mode

		Computer Analysis	Experimentally Identified
Frequency (Hz)		7.7925	7.9102
Mode Shape ratios	1	0.5173	0.4984
	2	0.8707	0.8838
	3	1.1321	1.1131
	4	1.2674	1.2753
	5	1.2195	1.2118
	6	1.0000	1.0000
	7	0.6380	0.6190

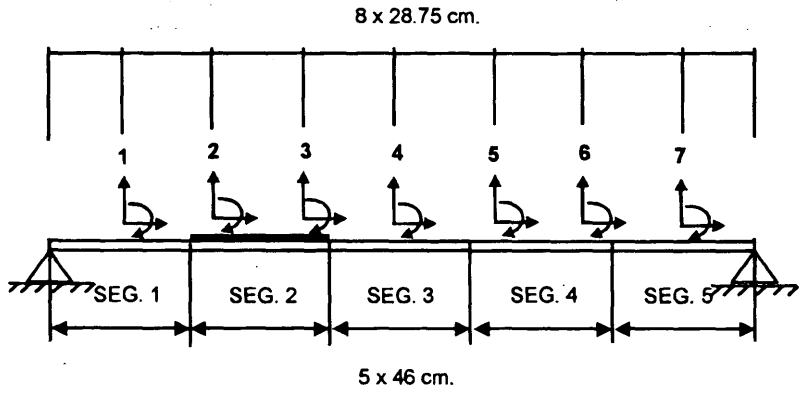

FIGURE 4 Computer model of the tested beam.

Then, by employing the proposed method for the modal parameters calculated for the numerical model and given in the first column of Table 1, the segmentary stiffness parameters of the numerical model were estimated and given in Table 2. In this table the actual segmentary stiffness parameters are given in the first column, and the results obtained without using any weighting or coordinate transformation are presented in the second column. In the fourth column, the results were produced by using the sensitivity-based coordinate transformation defined in Equation 4. In the third and fifth columns, percent differences of the obtained values are given.

Similarly, the segmentary stiffness parameters of the tested laboratory model were estimated by employing the proposed method for the modal parameters defined in the second column of Table 1. The results are presented in Table 3 using the same pattern as that used for Table 2. However, to produce the results presented in the fourth column in addition to the sensitivity-based coordinate transformation given in Equation 4, the weighting that reflects the relative confidence was used. The following upper and lower bounds (Equation 1) were set for the segmentary stiffness parameters:

$$0 < E_i \leq 1.5xE \qquad i = 1, \ldots, 5$$

The following initial values were estimated for unknown stiffness parameters:

$$E_{oi} = E \qquad i = 1, \ldots, 5$$

TABLE 2 Segmentary Stiffness Values × 10 kN/cm²: Numerical Model

Segment No.	Model (1)	Identified (2)	100x[(2)-(1)]/(1) (3)	Identified (4)	100x[(4)-(1)]/(1) (5)
1	2100	2398.9	14.23	2179.8	3.80
2	3482	2897.5	-16.79	3273.5	5.99
3	2100	2143.0	2.05	2110.2	0.49
4	2100	2004.1	4.57	2015.8	-4.00
5	2100	2102.3	0.11	2100.8	0.04

TABLE 3 Segmentary Stiffness Values × 10 kN/cm²: Laboratory Model

Segment No.	Model (1)	Identified (2)	100x[(2)-(1)]/(1) (3)	Identified (4)	100x[(4)-(1)]/(1) (5)
1	2100	2868.0	36.57	2199.8	4.75
2	3482	3578.2	2.76	3382.0	2.96
3	2100	2215.6	5.50	2273.6	8.27
4	2100	1995.0	-5.00	2033.2	3.18
5	2100	2464.2	17.34	2173.0	3.48

The results presented in Tables 2 and 3 showed the following:

1. That the proposed method works efficiently for the identification of the stiffness changes and successfully finds their locations and
2. That the sensitivity-based coordinate transformation presented in Equation and 4*a* and *b* effectively cures the accuracy and stability of the solutions.

LOCALIZED DAMAGE DETECTION METHOD

In the second phase, only the bridge members located in a segment for which global stiffness degradation is identified are instrumented properly for the strain measurements. However, for this case, in addition to the strain measurement axle loads and spacings, the location of the first axis of locomotive along the bridge and the train speed must be measured in the course of train passage.

After the static component of the recorded strain data is obtained, it is converted to stress to compare with the others coming from the computer analyses. To be able to compare properly both stress traces obtained from the measured strain data and the computer analysis, recorded data for the train movement must be reflected in the computer analysis to maintain a consistent rate of the movement of the train load on the bridge computer model. After the stress traces coming from the computer analysis and the recorded strain data are compared the damaged members are easily identified.

APPLICATION TO EXISTING RAILWAY BRIDGE

The field application of the procedure involved Çerkezköy Railway Bridge, a single span, single curved-track railroad bridge, 50 m long owned and operated by the Turkish State Railways Administration. The bridge structure consists of a single-deck steel-riveted truss. The bridge is part of the Istanbul-Edirne main railway line connecting Turkey with other European countries and was originally designed and constructed by Fried-Krupp A.G. in 1937 on the Sivas-Erzurum railway line in midwestern to eastern Anatolia and later relocated on the Istanbul-Edirne railway line.

All the stress and free vibration analyses needed for this application were performed by employing COSMOS/M Finite Element Software (*13*). SA-102 model uniaxial and SSA-302 model triaxial Terra Technology-made servo-accelerometers were used to measure accelerations of the bridge caused by passenger or freight train passages that occurred during the test. The acceleration transducer placement plan that was used in the course of the test is given in Figure 5.

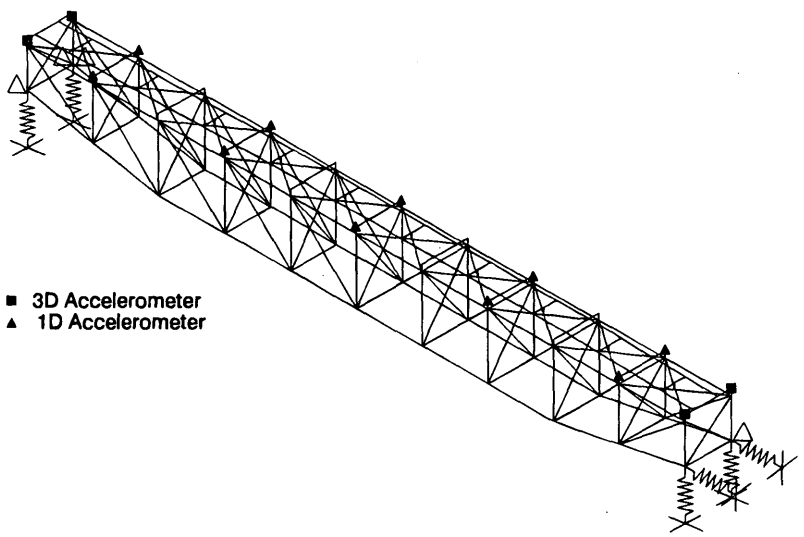

FIGURE 5 Acceleration transducer placement plan.

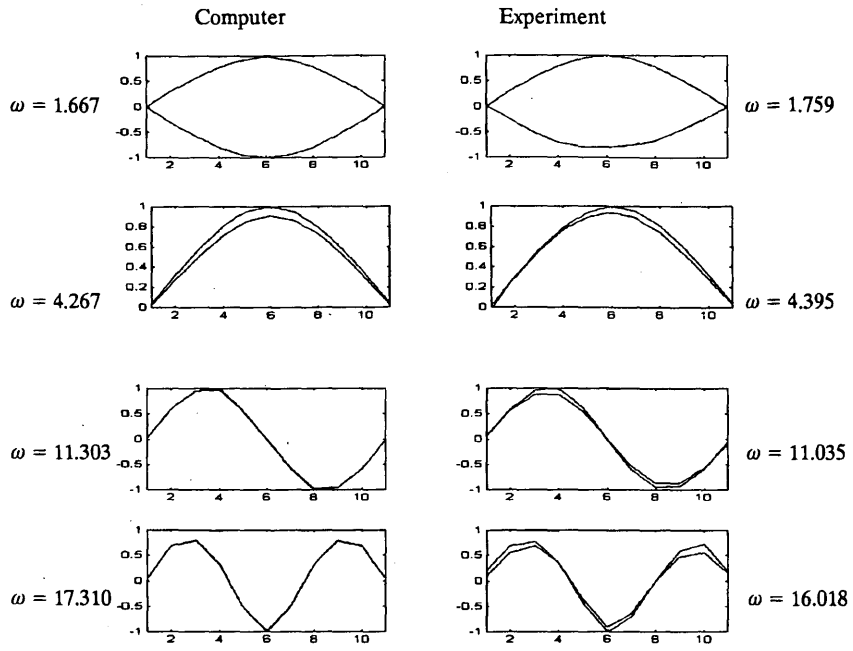

FIGURE 6 Comparison of the identified modes (all frequency values in hertz).

Because the bridge and train system constitute a coupled dynamic system having a time-dependent mass, the acceleration recordings following the time at which the train totally left the bridge were considered for this application.

Elevation views of the corresponding mode shapes are presented in Figure 6 along with the others obtained from computer analyses performed for the sophisticated bridge model.

Segmentary Stiffness Identification

Depending on the modal frequencies identified in the previous section and employing the method proposed for the global damage detection, segmentary stiffness parameters were identified and presented in Table 4 along with their percent variations with respect to the original values that were considered in the computer modeling.

TABLE 4 Identified Segmentary Stiffness Parameters

Number of Segment	$E_I \times 10^4$ [kN/cm^2]	$\frac{E_I - E_m}{E_m{}^a} \cdot 100$
1	1.9575	-6.79
2	2.0821	-0.85
3	1.6549	-21.20
4	2.1095	0.45
5	2.0152	-4.04
6	1.9775	-5.83
7	2.1161	0.77
8	1.7846	-15.02
9	2.1391	1.86
10	2.0130	-4.14

[a] $E_m = 2.1 \times 10^4$ kN/cm^2

It is clearly seen from Table 4 and Figure 7 that there is considerable stiffness degradation in Segments 3 and 8, which may be interpreted as a sign of existing damage. Similarly, for Segments 1, 5, 6, and 10 segments there are relatively small modulus of elasticity degradations.

Localized Damage Detection

After the noticeable global stiffness degradations for structural segments 1, 3, 5, 6, 8, and 10 were defined, selected bridge members located in these segments were instrumented for strain measurements. Strain readings were made through Hottinger Baldwin-made DS-5 model demountable strain transducers during passage of a DE24000 diesel locomotive during the test.

All the strain data recorded at various locations in the selected bridge members indicated in Figure 8 were filtered and converted to strain values for those members that seemed more informative. Obtained strain values are plotted in Figures 8 and 9 against time, corresponding to longitudinal locomotive positions, along with the others obtained from the computer analyses performed as mentioned in the preceding sections for the moving load model defined for the same locomotive passage.

It is clearly seen from the comparison of stress traces obtained from the data collected from the strain transducer locations on Members 30 and 32 (Figure 8) and 71 and 73 (Figure 9) that diagonal members having numbers 32 and 73, which are located in structural segments 3 and 8, respectively, work only for tension forces. They do not take compression force. As is seen from Figures 8 and 9, the stress trace peak for Members 30 and 71 in the region of compression has approximately the same value as the stress trace peak for Members 32 and 73 located in the region of tension, when the test locomotive is approaching from the Istanbul side. The same situation is valid for the test locomotive passage from the Edirne side to Istanbul. This abnormal working mechanism is caused by the existing loosening of the weak riveted joints connecting the upper chord members to Members 32 and 73.

From the observation of Figure 9 that demonstrates the stress traces obtained from the test data captured from the strain transducer locations on Members 39 and 80, which are located in Structural Segments 5 and 10, respectively, and obtained from the computed stress values, it is clearly seen that there is an obvious discrepancy between the stress traces obtained from the test and computer analyses. This abnormal behavior is caused by an improper working mechanism, which is exhibited by these members and is also the sign of existing joint loosening. Findings for Structural Segments 1 and 6 were similar to those obtained for Segments 5 and 10.

CONCLUSIONS

The following conclusions can be drawn from this study:

1. The global damage detection procedure developed in this study can be an effective tool for enhancing periodic bridge inspection and global damage identification.
2. If it is followed by the local damage detection procedure discussed in this study, localization of the globally identified damage is possible without using a large number of strain transducers.
3. The key to the efficiency of the method can be expressed as follows:
   a. The needed data can be recorded without closing the bridge to daily traffic and
   b. Current train traffic can be used as the excitation and loading mechanism; that is, no special loading vehicle is needed.

ACKNOWLEDGMENT

This paper is based on the research activities supported by NATO's Science for Stability Program under the contract name TU-BRIDGES. The authors wish to acknowledge numerous contributions from the Turkish Railways Administration.

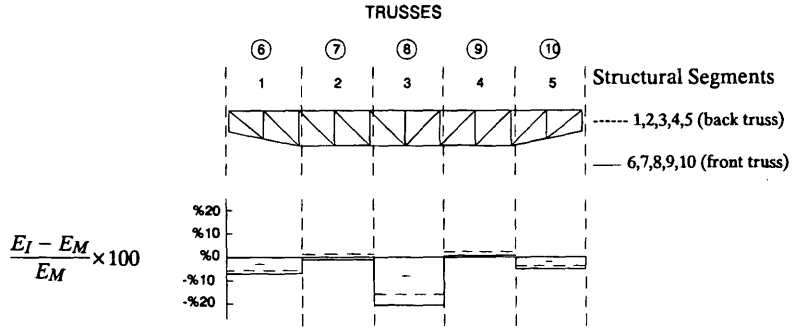

FIGURE 7 Characteristic regions and identified changes in modulus of elasticity.

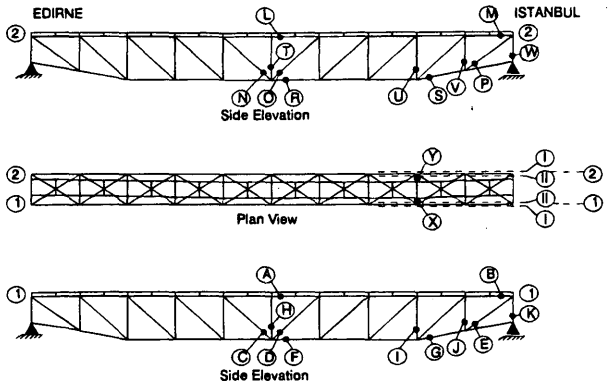

C

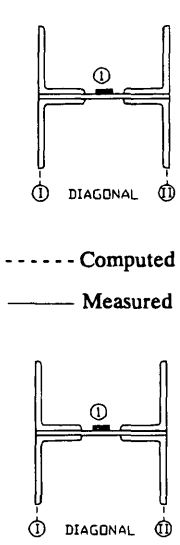

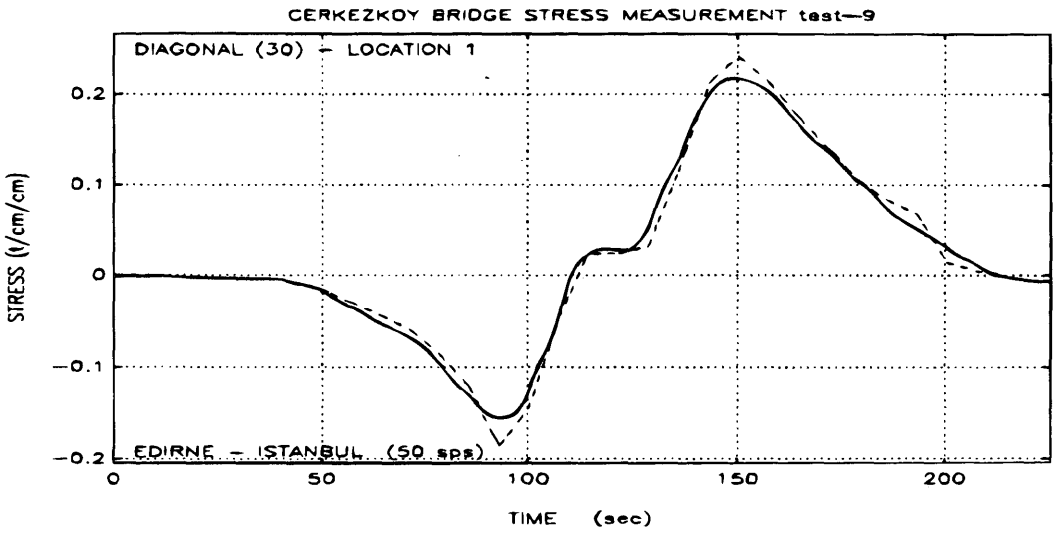

D

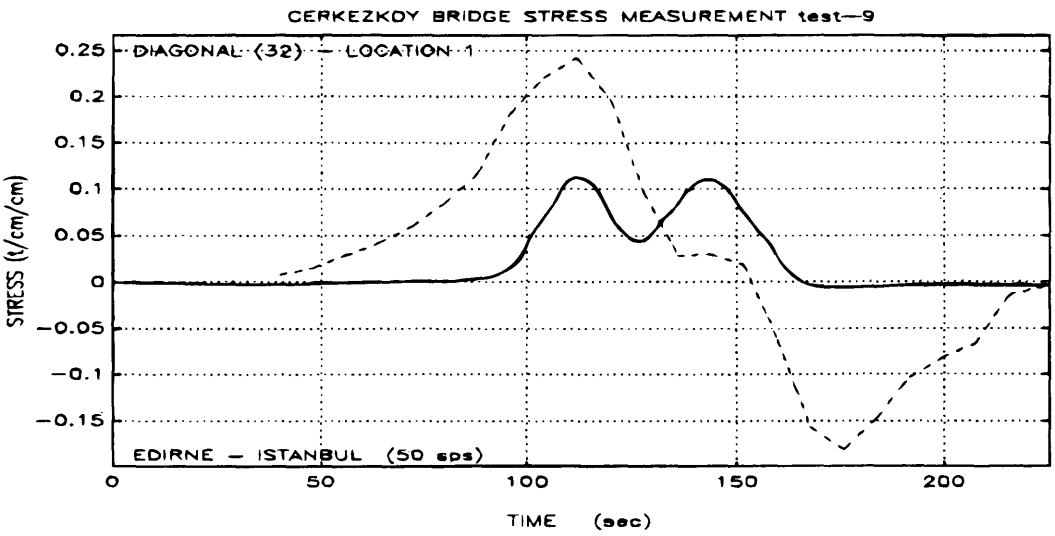

FIGURE 8 Computed and measured stress traces × 10 kN/cm².

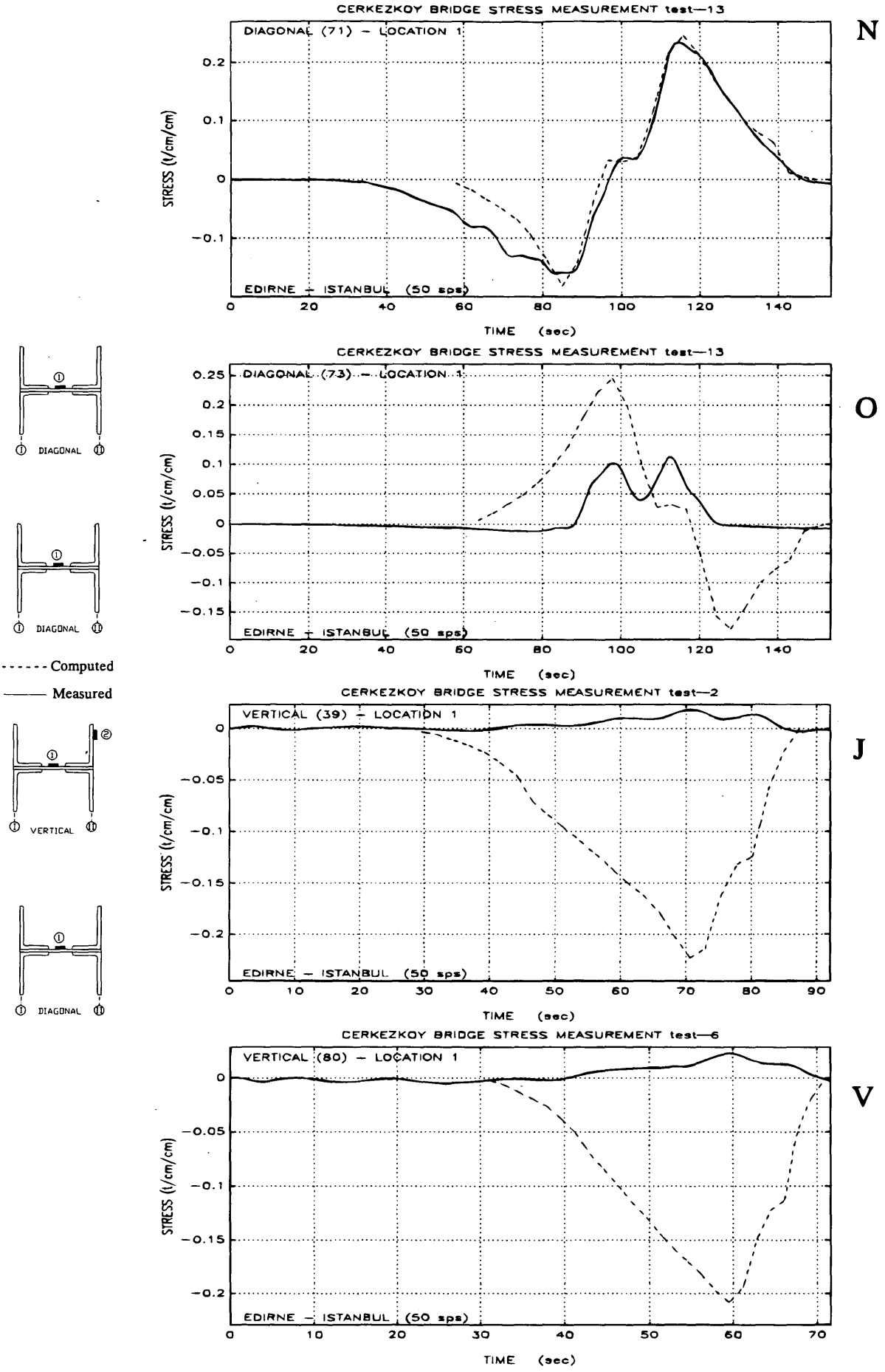

FIGURE 9 Computed and measured stress traces × 10 kN/cm².

REFERENCES

1. Bakht, B., and P. F. Csagoly. Testing of Perley Bridge. In *Ontario Ministry of Transportation and Communications*. RR207. Ontario, Canada, 1977.
2. Bakht, B., and P. F. Csagoly. Bridge Testing. In *Ontario Ministry of Transportation and Communications*. SRR-79-10. Ontario, Canada, 1979.
3. Billing, J. R. Dynamic Test of Bridges in Ontario, 1980: Data Capture, Test Procedures and Data Processing. In *Ontario Ministry of Transportation and Communications*. SRR-82-02. Ontario, Canada, 1982.
4. Mazurek, F., and J. T. DeWolf. Experimental Study of Bridge Monitoring Technique. *Journal of Structural Engineering* ASCE, Vol. 116, No. 9, Sept. 1990.
5. Felber, A. J. *Development of a Hybrid Bridge Evaluation System*. Ph.D. Dissertation. Department of Civil Engineering, University of British Columbia, Dec. 1993.
6. Safak, E. *Analysis of Recordings in Structural Engineering, Adaptive Filtering, Prediction and Control*. USGS Open-File Report 88-647. U.S. Geological Survey, 1988.
7. Bendat J. S., and A. G. Piersol. *Random Data: Analysis and Measurement Procedures*. Wiley Interscience, 1971.
8. Douglas, B. M., and W. H. Reid. Dynamic Tests and System Identification of the Bridges. *Journal of Structural Division*, ASCE, Vol. 108, 1982.
9. Fletcher, R. *Practical Methods of Optimization*, 2 vols. John Wiley & Sons, 1980.
10. Gill, P. E., W. Murry, and M. H. Wright. *Practical Optimization*. Academic Press, London, 1981.
11. Hock, H., and K. Schittowski. A Comparative Performance Evaluation of 27 Nonlinear Programming Codes. *Computing*, Vol. 30, 1983,
12. Bannan, M. R., and K. D. Hjelmstad. Parameter Estimation of Structures from Static Response, I. Computational Aspects. *Journal of Structural Engineering, ASCE*, Vol. 120, No.11, Nov. 1994.
13. COSMOS/M (386) Version 1.65 Finite Element System Software. *Structural Research and Analysis Corporation, Santa Monica, Calif. 1991.*

Publication of this paper sponsored by Committee on Dynamics and Field Testing of Bridges.